

- of 58.3°, C₁-C₂ bond length of 1.530 Å, C-H bond length 1.081 Å, and H-C-H angles of 113.8°.
- (11) Dewar and co-workers derived C₁-C₂ and C₂-C₃ bond lengths of 1.428 Å, C₁-C₂-C₃ bond angle of 62.6°, C₂-C₁-H bond angles of 119.7°, and H-C-C dihedral angles ~110° using the Simplex-MINDO/2 procedure (see ref 6).
 - (12) This MO description is different from that implied in ref 6 in which the nonbonded pair of electrons is depicted as occupying a 2p AO on C₂.
 - (13) In the geometry optimization calculations at 90° each H-C-C bond angle and H-C-C dihedral angle was optimized individually producing a structure with perfect C_{3v} symmetry. Final calculations at 90°, as well as those at 70 and 80°, were carried out by coupling symmetry related bond lengths, bond angles and dihedral angles.
 - (14) At 100° the H-C bond lengths, H-C-C bond angles, and H-C-C-C dihedral angles were individually optimized. After two complete cycles of optimization, the predicted geometry was approaching that with a plane of symmetry coincident with the C₁-C₂-C₃ plane. Instead of cycling further, the H₃-C₃ and H₄-C₃ bond lengths, H₃-C₃-C₂ and H₄-C₃-C₂ bond angles, and the H₃-C₃-C₂-C₁ and H₄-C₃-C₂-C₁ dihedral angles were symmetry coupled and optimized. This latter procedure was used at angles of 120-180°.
 - (15) For a thorough review of the stereochemical aspects of the ring opening of cyclopropylidenes see ref 7.
 - (16) Although in general the structures were optimized using the STO-3G minimal basis set, the results of the STO-3G calculations on the triplet energy surface indicated considerably greater contributions of higher spin states to the triplet wave function than in the 4-31G extended basis set as indicated by the value of $\langle S^2 \rangle$, particularly from 40% ring opening to allene. Therefore, 4-31G geometry optimization calculations were carried out on 1T, at 40% ring opening, and for bent planar allene. The geometries resulting from these calculations, however, were only negligibly different from the STO-3G optimized structures, and geometry optimization at the other points on the triplet surface were carried out using the STO-3G basis set with the final energies being calculated using the 4-31G extended basis set.
 - (17) P. Merlet, S. D. Peyerimhoff, R. J. Buenker, and S. Shih, *J. Am. Chem. Soc.*, **96**, 959 (1974).
 - (18) Incorporation of Cl in the calculations for the cyclopropyl cation resulted in only slight lowering of the activation energy, 1.6 to 1.3 kcal/mol for the disrotatory process and 86.3 to 78.5 kcal/mol for the conrotatory process.
 - (19) Because of the small effect of incorporation of Cl on the energies in the cyclopropyl cation calculations it was not considered worthwhile to incorporate Cl into the present calculations.
 - (20) The application of Koopmans' theorem to the cation and radical pair in ref 17 assumes that the two species have identical structures, i.e., planar cation and radical centers. However, in the case of the cyclopropyl radical, EPR²¹ and stereochemical studies²² involving the cyclopropyl radical have been interpreted in terms of a nonplanar radical center with a low energy barrier to inversion. This does not invalidate the comparisons made between 1T and the cyclopropyl radical as during the ring opening of the cyclopropyl radical planarity must be achieved along the reaction coordinate. Such a change in geometry would result in an increase in the activation energy for ring opening of the radical over that calculated on the basis of a planar radical in ref 17.
 - (21) R. W. Fessenden and R. H. Schuler, *J. Chem. Phys.*, **39**, 2147 (1963).
 - (22) K. Kobayashi and J. B. Lambert, *J. Org. Chem.*, **42**, 1254 (1977), and references cited therein.

Ab Initio Molecular Orbital Study of the Geometries, Properties, and Protonation of Simple Organofluorides¹

William L. Jorgensen* and Michael E. Cournoyer

Contribution from the Department of Chemistry, Purdue University, West Lafayette, Indiana 47907. Received January 12, 1978

Abstract: SCF calculations with minimal, STO-3G, and extended, 4-31G, basis sets have been used to study the geometries and properties of the simple alkyl fluorides, HF to *t*-BuF, and vinyl fluoride. Particular emphasis is placed on examining the corresponding protonated fluorides in order to better understand the gas-phase behavior of these species as well as to provide insight into the solvation of carbonium ions in a superacid medium such as liquid HF. In contrast to an earlier study of alkyl chlorides, computed properties for the protonated fluorides are poorly described with the minimal basis set calculations. This necessitates limited geometry optimization at the 4-31G level to obtain reasonable agreement with experimental proton affinities and carbonium ion-FH dissociation energies (ΔE_s). The small ΔE_s values (<8 kcal/mol) for protonated isopropyl and *tert*-butyl fluorides account for the inability to observe these ions in ICR experiments and provide evidence for the weak solvation of secondary and tertiary carbonium ions in superacid solutions. It is also found that an HF binds to bisected ethyl cation more strongly than the bridged ethyl cation by 4 kcal/mol. Although this is consistent with previous work, the conclusion could be modified by a more sophisticated theoretical treatment. As an exception, vinyl fluoride is predicted to protonate on carbon rather than fluorine; the reason is illuminated by a simple frontier orbital analysis. Various correlations involving the properties of the fluorides are noted, while differences in the behavior of chlorides and fluorides can usually be ascribed to the greater basicity and weaker electronegativity of chlorine.

The current interest in chemistry in the gas phase² and in superacid media³ prompted a series of theoretical studies on the properties and protonation of alkyl chlorides.⁴ Both semiempirical and ab initio molecular orbital calculations were used to explore the origins of variations in proton affinities and in the interactions between carbonium ions and HCl. The present work extends the analyses to alkyl fluorides and their protonated analogues. This order of presentation may at first seem unusual; however, it resulted from the fact that neither semiempirical nor ab initio calculations with minimal basis sets yield adequate descriptions of protonated fluorides, whereas both approaches are suitable for the study of neutral and protonated alkyl chlorides.⁴ As discussed below, greater sophistication is necessary in the ab initio calculations to obtain energetic results in reasonable agreement with experiment for protonated alkyl fluorides.

The detailed purposes of this paper are: (1) to examine the structures and thermodynamic stability of protonated alkyl

fluorides in the gas phase; (2) to determine the extent of interaction between various carbonium ions and HF as a primitive model for solvation in a superacid medium; and (3) to seek out correlations involving the properties of the fluorides and to compare the results with similar data for chlorides. The molecules treated are the simple alkyl fluorides, HF to *t*-BuF, vinyl fluoride, and their protonated derivatives. The method of analysis employs single determinant, ab initio molecular orbital calculations with both a minimal STO-3G^{5a} basis set and the extended, split-valence 4-31G^{5b} basis. The computations were performed using the GAUSSIAN/74 program⁶ on the CDC/6500 system at Purdue.

Several significant findings were made in the course of this research. Consistent with other studies of the protonation of bases containing first-row elements,⁷ the protonated fluorides are much too bound at the STO-3G level which is witnessed by proton affinities (PAs) that are too high by 40-60 kcal/mol. The consequent errors in the geometries of the ions cause

Table I. Calculated and Experimental Geometries for Neutral Fluorides^a

molecule	symmetry	parameter	STO-3G	exptl
HF	$C_{\infty v}$	$r(\text{F-H})$	0.956	0.917 ^b
CH ₃ F	C_{3v}	$r(\text{C-F})$	1.387	1.384 ^c
CH ₂ CHF	C_s	$r(\text{C-F})$	1.352	1.348 ^d
		$r(\text{C-C})$	1.313	1.333
		$\angle\text{CCF}$	124.6	121
		$r(\text{C-F})$	1.387	1.375 ^d
CH ₃ CH ₂ F staggered	C_s	$r(\text{C-F})$	1.387	1.375 ^d
		$r(\text{C-C})$	1.550	1.540
		$\angle\text{CCF}$	110.7	
(CH ₃) ₂ CHF,	C_s	$r(\text{C-F})$	(1.39, 1.43 ^e)	1.43 ^{d,e}
(CH ₃) ₃ CF	C_{3v}	$r(\text{C-C})$	(1.54)	1.516
		$\angle\text{CCC}$	(109.5)	112.7

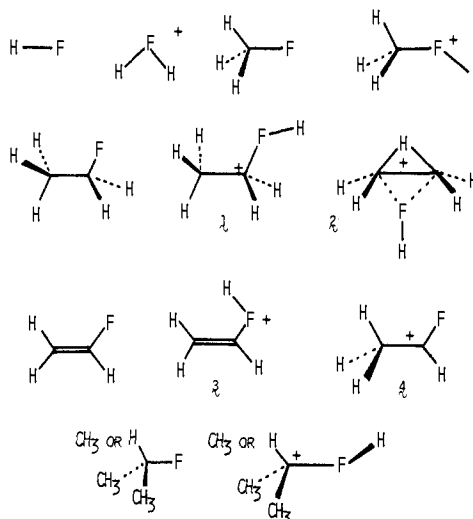
^a Bond lengths in ångströms; bond angles in degrees. ^b G. A. Knipers, D. F. Smith, and A. N. Nielsen, *J. Chem. Phys.*, **25**, 275 (1956). ^c C. Costain, *ibid.*, **29**, 864 (1958). ^d L. E. Sutton, *Chem. Soc., Spec. Publ.*, No. **11** (1958); No. **18** (1965). ^e Data for *t*-BuF.

4-31G values for the PAs and carbonium ion-HF dissociation energies (ΔE_s 's) to be too low when the STO-3G geometries are used. A remedy is to partially optimize the geometries, particularly the C-F distances, with the extended basis. The resulting PAs and ΔE_s 's are then in good agreement with experiment and reveal some interesting features. First, the PAs and ΔE_s 's are 10–20 kcal/mol lower for fluorides than for corresponding chlorides, while both series reveal correlations of the PAs with Taft's σ^* constants and with the charge on the XH fragment in RXH^+ where X = F, Cl. The ΔE_s values for *i*-PrFH⁺ and *t*-BuFH⁺ are so low (<8 kcal/mol) that the inability to observe such species in ICR experiments⁸ can be rationalized. In addition, the same effect is consistent with the weak solvation of secondary and tertiary carbonium ions in superacid media. The ΔE_s for the interaction of HF with the bisected and bridged ethyl cations indicates that protonated ethyl fluoride should undergo facile degenerate rearrangement. Finally, the preference for protonation of vinyl fluoride on carbon rather than fluorine is shown to agree with straight-forward frontier orbital concepts.

Results for the Neutral Fluorides

The molecules that were treated in this work are illustrated in Figure 1. The geometries for the four smallest species were fully optimized by Pople et al.¹⁰ at the STO-3G level. The larger neutral fluorides were handled using a combination of standard bond lengths and angles¹¹ and limited geometry optimization with the STO-3G basis set. The standard procedure of sequential optimization of variables using a quadratic least-squares program was followed.⁶ Convergence was generally obtained within two or three cycles. The resulting bond lengths and angles are anticipated to be accurate to within ± 0.01 Å and $\pm 1^\circ$.

Optimized parameters for the neutral molecules are compared with experiment in Table I. Overall, the agreement is very good, particularly for C-F bond lengths. In fact, the geometries of the fluorides are somewhat better predicted than for chlorides in which case STO-3G calculations consistently overestimate C-Cl bond lengths by 0.02–0.04 Å.^{4b} It may also be noted that the standard C-F bond lengths recommended by Pople and Gordon¹¹ are slightly too short. Based on the data in Table I, the standard value for a sp^3 C-F bond should be changed from 1.36 Å¹¹ to 1.38 Å and a sp^2 C-F bond is better represented as 1.35 Å than 1.33 Å.¹¹ In this spirit the C-F length for *i*-PrF was taken as 1.39 Å for the calculations and the experimental value of 1.43 Å was used for the C-F bond in *t*-BuF. Since the geometries determined in the minimal basis set calculations for the neutral species were reasonable, further optimization was not performed with 4-31G calculations. Rather, only one 4-31G calculation was made at the final STO-3G geometry for each neutral molecule except *t*-BuF for

**Figure 1.** Structures of neutral and protonated fluorides.

reasons discussed below. The total energies computed for all the molecules in this study are collected in Table II.

The ionization potentials (IPs) calculated from Koopman's theorem and dipole moments for the neutral fluorides are listed along with experimental values in Table III. As in the case of chlorides, the low IPs for the fluorides determined using STO-3G are significantly improved by the extended basis. For both theoretical approaches, however, the ordering of the IPs is correct and the relative values are reasonable. The IPs for the alkyl fluorides are found to correlate with Taft's σ^* polar constants¹² for the alkyl groups according to

$$\text{IP (STO-3G)} = 2.880\sigma^* + 11.229 \text{ eV} \quad (1)$$

with a standard deviation of 0.12 eV. Similar relations hold for other alkyl halides and alcohols.^{4,13} As previously discussed, the correlations are not general because they do not apply to polyfunctional and cyclic derivatives.⁴ The agreement for the acyclic alkyl compounds can largely be attributed to the roughly constant increment of 0.1 σ^* unit in going from methyl to ethyl to isopropyl to *tert*-butyl. The effect of sequentially replacing each hydrogen in a methyl substituent with a methyl group may reasonably be expected to be constant in many instances.

Dipole moments are computed to be too small with the STO-3G basis, while the tendency of 4-31G calculations to overemphasize the polarity of molecules is again apparent.^{4b,7} Nevertheless, both approaches reproduce the interesting feature that the dipole moments of alkyl fluorides are relatively insensitive to variations in the alkyl group. Thus, experimen-

Table II. Calculated Total Energies (au)

molecule	STO-3G (opt) ^{a,d}	4-31G ^b	4-31G (opt) ^{c,d}
HF	-98.572 85	-99.886 13	-99.887 29
HFH ⁺	-98.864 11	-100.074 69	-100.077 87
CH ₃ F	-137.169 06 ^e	-138.856 86 ^e	
CH ₃ FH ⁺	-137.483 22 ^e	-139.090 85 ^e	-139.101 84
CH ₂ CHF	-174.532 23	-176.649 17	
CH ₂ CHFH ⁺	(-174.797 83)		-176.879 84
CH ₃ CHF ⁺	(-174.893 14)		-176.921 36
CH ₃ CH ₂ F	-175.753 24	-177.842 30	
CH ₃ CH ₂ FH ⁺	-176.081 41	-178.090 73	-178.105 21
c-CH ₃ CH ₂ FH ⁺	(-175.971 98)		-178.087 78
(CH ₃) ₂ CHF	-214.336 94	-216.827 30	
(CH ₃) ₂ CHFH ⁺	(-214.606 42)		-217.106 48
(CH ₃) ₃ CF	-252.918 51		
(CH ₃) ₃ CFH ⁺	(-253.218 01)		

^a STO-3G results using STO-3G optimized geometries except values in parentheses which are STO-3G results using 4-31G optimized geometries. ^b 4-31G results using STO-3G optimized geometries. ^c 4-31G results using 4-31G optimized geometries. ^d Extent of optimization varies; see text for details. ^e From ref 10.

Table III. Ionization Potentials and Dipole Moments

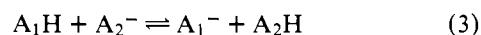
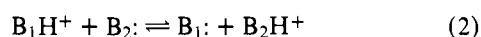
molecule	STO-3G	4-31G ^a	exptl
Ionization Potentials (eV)			
HF	12.63	16.99	16.0 ^b
CH ₃ F	11.38	14.26	12.5 ^b
CH ₂ CHF	8.50	10.55	10.4 ^b
CH ₃ CH ₂ F	10.86	13.42	12.0 ^d
(CH ₃) ₂ CHF	10.54	12.82	11.1 ^e
(CH ₃) ₃ CF	10.46		
Dipole Moments (D)			
HF	1.28	2.29	1.82 ^c
CH ₃ F	1.16	2.50	1.85
CH ₂ CHF	0.90	2.10	1.43
CH ₃ CH ₂ F	1.21	2.46	1.94
(CH ₃) ₂ CHF	1.24	2.40	
(CH ₃) ₃ CF	1.31		1.96

^a 4-31G results using the STO-3G optimized geometries. ^b H. M. Rosenstock, K. Draxl, B. W. Steiner, and J. T. Herron, *J. Phys. Chem. Ref. Data, Suppl. 1*, **6** (1977). ^c R. D. Nelson, D. R. Lide, and A. Maryott, *Natl. Bur. Stand. (U.S.), Circ.*, No. **10** (1967). ^d C. A. McDowell and B. G. Cox, *J. Chem. Phys.*, **22**, 946 (1954). ^e From ref 8a.

tally the difference in dipole moments between HF and *t*-BuF is only 0.14 D, while the corresponding figure for chlorides is 1.05 D.^{4b} The variation can be attributed to the greater polarizability of chlorine than fluorine. Analogously, bromine should be even more responsive to its electronic environment; this is supported by dipole moments of 0.82 and 2.21 D for HBr and *i*-PrBr, respectively.¹⁴

Results for Protonated Fluorides

One of the important contributions of nonempirical molecular orbital calculations has been the detailed description of the geometries of ions in the gas phase.¹⁵ Such information has so far proved difficult to obtain by experiment owing to the difficulty in obtaining sufficient ion concentrations. Consequently, support for the theoretical predictions comes from indirect means such as NMR studies in superacid where solvent effects are often assumed to be minor³ and from comparisons with the energetics of gas-phase reactions. In the latter category, both relative proton affinities¹⁶ and relative acidities¹⁷ may be determined by studying the position of equilibria as in



using ion cyclotron resonance or high-pressure mass spectrometry. Then, with the aid of more complete information on a few reference compounds, it has been possible to assign absolute PAs and acidities to a wide variety of organic molecules.^{16,17}

In the present context, the key data available on protonated fluorides are the PAs that have been determined by Beauchamp and co-workers.^{2a,8,9} Specifically, PAs have been reported for HF,^{9a} CH₃F,^{2a} C₂H₅F,^{2a} and C₂H₃F;^{8a} however, protonated isopropyl fluoride has not been observed upon ionization of (CH₃)₂CHF in ICR experiments.⁸ The theoretical results discussed below indicate even less likelihood for detecting protonated *tert*-butyl fluoride. In any event, if agreement was found between the experimental and calculated PAs for fluorides, increased confidence in the reliability of the computed structures for the protonated species would be obtained. A survey of the literature reveals that such assurance is not provided by minimal basis set calculations on the protonation of first-row bases. For example, STO-3G calculations with complete geometry optimization find the PAs of water,⁷ HF,¹⁰ and CH₃F¹⁰ to be too high by 56, 61, and 43 kcal/mol, respectively. However, when the geometries of water and H₃O⁺ are optimized at the 4-31G level, the computed PA is reduced to 183 kcal/mol,^{7b} which is in substantially better agreement with the experimental value of 170.3 kcal/mol.^{16a} Interestingly, 4-31G calculations predict a planar geometry for H₃O⁺ with *r*(O-H) = 0.964 Å. There are no gas-phase data available on this point; however, crystal structures, STO-3G results, and the near Hartree-Fock limit calculations of Kollman and Bender prefer a slightly pyramidalized geometry with ∠HOH = ca. 112°. The inversion barrier calculated by Kollman and Bender is very small (1.9 kcal/mol) and their value of 0.963 Å for *r*(O-H) is in excellent agreement with the 4-31G estimate.

Thus, it is apparent that to obtain good PAs and Δ*E*_s's for protonated fluorides, some geometry optimization with 4-31G calculations should be performed for the ions. A problem with this approach is the expense which necessitates some choice in the important parameters to be optimized. The details of the geometry optimizations for each species are discussed below in addition to the energetic results. Overall, the 4-31G computations are in good agreement with experiment and the critical parameter in the optimizations is revealed to be the C-F distance. Summaries of the computed PAs and geometries are presented in Tables IV and V. Table IV also compares the computed and experimental carbonium ion-FH dissociation energies (Δ*E*_s's) which are defined by eq 4 and are related to PAs by eq 5.¹⁹ An equivalence between changes in enthalpies

Table IV. Proton Affinities and Cation-FH Dissociation Energies

molecule	STO-3G (opt) ^e	4-31G	4-31G (opt)	exptl
Proton Affinities (kcal/mol)				
HF	182.8	118.4	9/6	112 ^a
CH ₃ F	197.2	146.9	153.6	151 ^b
CH ₂ CHF	230.1 ^f (226.5)		170.8	171 ^c
CH ₃ CH ₂ F	206.0 (163.8)	155.9	165.0	163 ^b
(CH ₃) ₂ CHF	(169.2)		175.2	
(CH ₃) ₃ CF	(188.0)			
Cation-FH Dissociation Energies, ΔE_s (kcal/mol)				
HFH ⁺	182.8	118.4	119.6	112 ^a
CH ₃ FH ⁺	82.2	20.9	27.8	36 ^b
CH ₃ CHF ⁺	(97.2)		36.2	38 ^{c,d}
CH ₂ CHF ⁺	(37.4)		10.2	
CH ₃ CH ₂ FH ⁺	63.1 (20.9)	6.1	15.1	13 ^{b-d}
c-CH ₃ CH ₂ FH ⁺	(5.8)		11.0	
(CH ₃) ₂ CHF ⁺	(3.7)		7.4	
(CH ₃) ₃ CFH ⁺	(3.8)			

^a From ref 9a. ^b From ref 2a. ^c From ref 8. ^d F. P. Lossing and G. P. Semeluk, *Can. J. Chem.*, **48**, 955 (1970); F. P. Lossing, *ibid.*, **49**, 357 (1971); **50**, 3973 (1972). ^e Values in parentheses are STO-3G results using the partially optimized 4-31G geometries. ^f Using data from ref 35a.

Table V. Calculated Geometries for Protonated Fluorides^a

molecule	symmetry	parameter	STO-3G	4-31G
H ₂ F ⁺	C _{2v}	r(F-H)	0.974	0.969
		\angle HFH	112.0	125.4
CH ₃ FH ⁺	C _s	r(C-F)	1.486 ^c	1.822
		r(F-H)	0.968	(0.968)
		\angle CFH	114.5	(114.1)
		\angle HCF	103.0, 105.9	96.7
CH ₂ CHF ⁺	C _s	r(C-H)	1.100, 1.101	(1.10)
		r(C-F)		1.850
		r(C-C)		(1.281)
		\angle CCF		103.7
CH ₃ CHF ⁺	C ₁	r(C-F)	1.275 ^d	1.275
		r(C-C)	1.510 ^d	(1.45)
		\angle CCF	122.4 ^d	(120.0)
		r(C-F)	1.518	2.137
CH ₃ CH ₂ FH ⁺ staggered	C _s	r(C-C)	1.533	(1.484)
		r(F-H)	0.966	(0.966)
		\angle CCF	103.4	(103.4)
		\angle CFH	114.7	(114.7)
		\angle C2C1H	115.9	(121.6)
		\angle HC2C1H	67.6	(88.2)
CH ₃ CH ₂ FH ⁺ bridged	C _{2v}	r(X-F) ^b		2.644
		r(F-H)		(0.966)
		r(C-C)		(1.403)
		\angle XFH ^b		180.0
(CH ₃) ₂ CHF ⁺	C ₁	r(C-F)		2.809
		r(C-C)		(1.500)
		r(F-H)		(0.966)
		\angle C1C2F		(103.4)
		\angle C1C2FH		(180.0)

^a Bond lengths in ångströms; bond angles in degrees. Values in parentheses are assumed. ^b X is the midpoint of the CC bond. ^c From ref 10. ^d From ref 35a.

and energies has been assumed, as usual, in order to ease comparisons with the experimental data.

$$\Delta E_s = E(R^+) + E(HF) - E(RFH^+) \quad (4)$$

$$\Delta E_s = E(R^+) + E(HF) + PA(RF) - E(RF) - E(H^+) \quad (5)$$

$$PA(RF) = E(RF) + E(H^+) - E(RFH^+) \quad (6)$$

H₂F⁺ and CH₃FH⁺

For H₂F⁺ use of the STO-3G geometry in a single 4-31G calculation reduces the PA of HF to 118.4 kcal/mol, which is in respectable accord with the experimental number, 112

kcal/mol.²⁰ Optimization of the geometry with the extended basis does little to the HF distance, while the HFH angle widens from 112 to 125° as shown in Table V. The energetic effect is slight, so the PA only rises to 119.6 kcal/mol (Table IV).

The STO-3G geometry for CH₃FH⁺ that was determined by Pople¹⁰ is summarized in Table V and corresponds to the staggered conformer illustrated in Figure 1. Several features of this structure were used in the limited 4-31G optimizations, specifically, the C-H bond lengths (1.10 Å), the CFH angle (114°), the F-H bond length (0.968), and the essential equivalence of the HCF angles. The C-F distance and the

HCF angle were then reoptimized with 4-31G calculations. This has a profound effect on the C–F bond length, which increases by 0.34 Å to 1.822 Å. Simultaneously the methyl group flattens to a HCF angle of 96.7°. Thus, the 4-31G calculations are clearly assigning more $\text{H}_3\text{C}^+\cdots\text{FH}$ character to the structure than STO-3G. Ab initio calculations with an even larger basis set would be needed to test whether this effect is over-emphasized by the tendency of 4-31G results to exaggerate the polarity of molecules; however, the 4-31G estimate of the PA for methyl fluoride, 153.6 kcal/mol, is within the error limits for the experimental value, 151 kcal/mol.^{2a} These results also show that the major improvement in the PAs comes from the change in basis set from STO-3G to 4-31G rather than geometry optimization at the 4-31G level. However, the geometry optimization is necessary to obtain good estimates of ΔE_s (Table IV).

Staggered and Bridged $\text{C}_2\text{H}_5\text{FH}^+$

The two structures considered for protonated ethyl fluoride are shown in Figure 1 and may be described as staggered (**1**) and doubly bridged (**2**). The two structures correspond to HF interacting with the classical and nonclassical forms of the ethyl cation. The accuracy of this analogy is stressed by noting that the experimental ΔE_s for $\text{C}_2\text{H}_5\text{FH}^+$ is only 13 kcal/mol (Table IV), i.e., only 13 kcal/mol is required to fragment the species to separated C_2H_5^+ and HF in the gas phase.

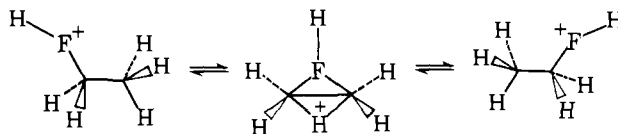
The geometry of **1** was extensively optimized at the STO-3G level as summarized in Table V. CH lengths of 1.09–1.10 Å and tetrahedral C1C2H angles were assumed. The CF length of 1.518 Å and the overestimation of the PA by 43 kcal/mol indicate that the computed structure is too covalently bound. Although a single 4-31G calculation at the STO-3G geometry improves the PA to 155.9 kcal/mol (exptl, 163 kcal/mol), the computed ΔE_s , 6.1 kcal/mol, is unacceptably low.

In view of the analogy described above, it seemed reasonable to attempt to approximate the structure of $\text{C}_2\text{H}_5\text{FH}^+$ as the bisected ethyl cation plus FH. This was done at the 4-31G level and the CF bond length was computed to be 2.137 Å, 0.62 Å longer than the STO-3G value. For these calculations, the structure of the ethyl cation was taken as the STO-3G optimized result¹⁰ and the remaining parameters were obtained from the STO-3G findings for $\text{C}_2\text{H}_5\text{FH}^+$.¹⁹ The assignments are recorded in Table V. The PA, 165 kcal/mol, and the ΔE_s , 15.1 kcal/mol, from the 4-31G calculations are in excellent agreement with the experimental estimates and lend support to the model. Clearly, complete optimization would make these values somewhat more positive, though the effect is not anticipated to be large owing to the low experimental ΔE_s .

MINDO/3 calculations for bridged ethyl cation interacting with HCl led to the chlorine analogue of **2** as the lowest energy form.^{21a} Using the STO-3G geometry¹⁰ of bridged C_2H_5^+ and the same F–H distance as in **1**, the geometry of **2** was optimized in C_s symmetry with 4-31G computations. In contrast to the MINDO/3 results on the chlorine analogue, **2** is found to have C_{2v} symmetry. The distance between the fluorine and the midpoint of the CC bond is 2.644 Å, which yields a CF distance of 2.735 Å.

The energy of **1** is found to be 10.9 kcal/mol lower than for **2** from the 4-31G calculations. This difference is certainly overestimated since the energetic favoring of the bisected ethyl cation over the bridged isomer is reversed from 7 kcal/mol at the 4-31G level to –1 kcal/mol using the 6-31G** basis and to –9 kcal/mol when correlation effects are also included.²² Clearly, the addition of polarization functions and corrections for the correlation energy benefit cyclic structures more than acyclic isomers. The effects are large enough that **2** may well be lower in energy than **1**. Nevertheless, the energy difference should be small (<5–10 kcal/mol), so **1** and **2** are expected to undergo facile degenerate rearrangement and hydrogen

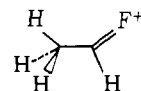
scrambling. A species like **2** with TsOH replacing FH may account for the deuterium scrambling during the reaction of $\text{CH}_3\text{CD}_2\text{OTs}$ with FSO_3H .^{21b}



CH_2CHF^+ and CH_3CHF^+

Two structures were considered for protonated vinyl fluoride corresponding to protonation on fluorine (**3**, CH_2CHF^+) and on carbon (**4**, CH_3CHF^+). Two other isomers worthy of mention are the hydrogen and fluorine bridged possibilities. It is not likely that the former is an energy minimum, since Clark²³ found it to be 27.3 kcal/mol above **4** in energy using ab initio calculations. It seems even less reasonable that the fluoronium ion would be lower in energy than the 1-fluoroethyl cation (**4**). Hehre has studied these isomers except **3** with STO-3G and 4-31G calculations and found **4** to be lowest in energy.³⁵ Furthermore, the following results are fully consistent with **4** being the species formed upon protonation of vinyl fluoride.

Standard geometrical parameters¹¹ including a C1–C2 length of 1.45 Å were used for **4** except that the C–F bond length was optimized with 4-31G calculations. The resultant distance is 1.275 Å, which represents a contraction of 0.08 Å relative to the C–F separation in vinyl fluoride. This suggests some contribution from **5** as a resonance structure. As shown



in Table IV, the computed PA and ΔE_s are in excellent agreement with experiment when **4** is taken as the protonated species and the open vinyl cation is the reference carbonium ion.

The structure of **3** was adopted from vinyl cation plus FH, analogous to the case for $\text{C}_2\text{H}_5\text{FH}^+$ above. The C–F distance and the CCF angle were then optimized at the 4-31G level assuming that the fluorine is on the C2C1H bisector. The results are given in Table V. The PA and ΔE_s derived from this ion are 144.8 and 10.2 kcal/mol, respectively. This reflects that **3** is calculated to be 26.1 kcal/mol less stable than **4**. Even with liberal error limits due to the incomplete geometry optimizations, there is little doubt that **4** is the ion observed in Beauchamp's ICR experiments.⁸

It is instructive to analyze the preference for protonation on carbon vs. fluorine in vinyl fluoride from a frontier orbital standpoint.²⁴ The important interaction during protonation is anticipated to occur between the HOMO of the base and the empty 1s orbital of the proton. The HOMO is the out-of-phase combination of the π_{cc} bond orbital and the 2p AO on fluorine. The orbital is illustrated in Figure 2 as constructed from the STO-3G wave function.²⁵ Protonation should occur at the atom with the largest coefficient in the HOMO which is clearly C2. Thus, vinyl fluoride is predicted to both thermodynamically and kinetically prefer protonation on C2 rather than fluorine.²⁶

$(\text{CH}_3)_2\text{CHF}^+$ and $(\text{CH}_3)_3\text{CF}^+$

In view of the low ΔE_s for $\text{C}_2\text{H}_5\text{FH}^+$ and the greater stability of secondary and tertiary carbonium ions than C_2H_5^+ , it seems appropriate to treat $(\text{CH}_3)_2\text{CHF}^+$ and $(\text{CH}_3)_3\text{CF}^+$ as the corresponding carbocations plus HF. The STO-3G geometries of isopropyl and *tert*-butyl cations¹⁹ were used in the computations and the other parameters were adopted from the $\text{C}_2\text{H}_5\text{FH}^+$ results. The C–F bond length for $(\text{CH}_3)_2\text{CHF}^+$ optimized with 4-31G calculations and found to be

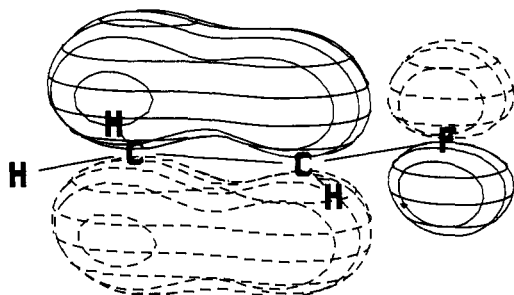
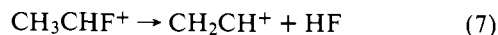


Figure 2. The highest occupied molecular orbital (HOMO) for vinyl fluoride.

2.81 Å. These computations were complicated by the flatness of the potential surface for C–F distances of 2.6–2.9 Å and slow SCF convergence. The latter trouble was overcome by using a damping procedure. The computed ΔE_s is 7.4 kcal/mol (Table IV).

It seemed difficult to attempt 4-31G calculations on $(\text{CH}_3)_3\text{CFH}^+$ owing to the problems for $(\text{CH}_3)_2\text{CHF}^+$ at large C–F distances. The projected computation time of 2 h per point on the CDC/6400 was also discouraging. Thus, only a STO-3G calculation was performed for $t\text{-BuFH}^+$ at $r(\text{C}-\text{F}) = 2.913$ Å. The latter figure was derived by adding the increase in the C–Cl distance in going from $i\text{-PrClH}^+$ to $t\text{-BuClH}^+$ ^{4b} to the C–F length in $i\text{-PrFH}^+$. As shown in Table IV, the STO-3G values of the ΔE_s 's for $\text{C}_2\text{H}_5\text{FH}^+$ and $(\text{CH}_3)_2\text{CHF}^+$ using the 4-31G geometries are in only fair agreement with the 4-31G estimates. The agreement is particularly poor for the ΔE_s of CH_3CHF^+ , which may be attributed to basis set truncation and correlation energy problems. Note that eq 7 is far fromisodesmic owing in particular to the protonation on carbon rather than fluorine.^{27,28}



The STO-3G estimate of 3.8 kcal/mol for the ΔE_s of $t\text{-BuFH}^+$ indicates that the assumed C–F distance (2.913 Å) is too short since the ΔE_s should be lower than for $i\text{-PrFH}^+$ owing to the greater stability of $t\text{-Bu}^+$ than $i\text{-Pr}^+$. It can be concluded that the ΔE_s values for $i\text{-PrFH}^+$ and $t\text{-BuFH}^+$ are similar and less than ca. 8 kcal/mol, i.e., comparable in energy to hydrogen bonding.

The low ΔE_s for $i\text{-PrFH}^+$ helps to explain the elusiveness of this species in ICR experiments at room temperature.⁸ Specifically, the ΔS for the fragmentation of a protonated haloalkane to a carbonium ion and HX may be estimated as roughly +18 cal/mol·K.²⁹ This requires a ΔE_s of at least 5.4 kcal/mol for the dissociation not to occur spontaneously at 300 K. Thus, the theoretical results described here predict that protonated isopropyl and *tert*-butyl fluorides should be sought in mass spectrometry experiments carried out at low temperature. Similarly, $t\text{-BuClH}^+$ should be elusive, while $i\text{-PrClH}^+$ is detectable.^{4b}



Proton Affinity Correlations

PAs for primary amines, alcohols, and alkyl halides have previously been found to correlate roughly with the σ^* values for the alkyl groups.⁴ The relation also holds for fluorides as shown in Figure 3. The data in the illustration for amines and alcohols are experimental results, while the PAs for chlorides and fluorides are from STO-3G and 4-31G calculations, respectively.⁴ As in the case of ionization potentials, the choice of σ^* for the abscissa is largely for convenience.

The data reveal several clear patterns. (1) The order of basicity is primary amines > alcohols > chlorides > fluorides, which is roughly opposite to the order of electronegativities for

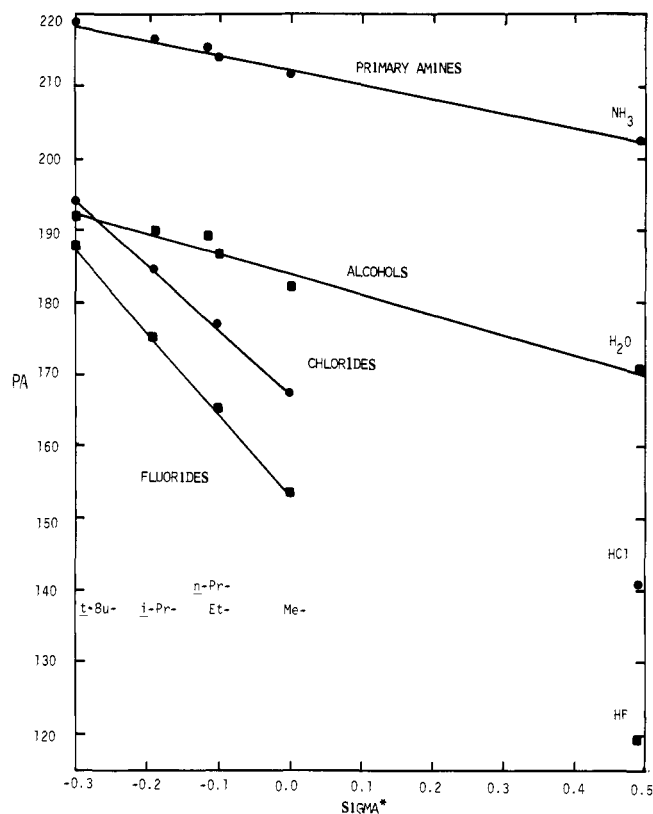


Figure 3. Correlation of PAs for alkyl derivatives with σ^* . Experimental data are shown for amines and alcohols. PAs for chlorides and fluorides are STO-3G and 4-31G results, respectively, except for the value for $t\text{-BuF}$ which is estimated from STO-3G results.

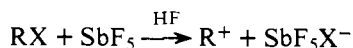
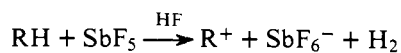
the corresponding heteratoms. Thus, PAs are generally expected to increase going from column 7A to 5A in the periodic table and going down a column. However, even this is not a global rule because the following order of PAs is known: $\text{NH}_3 > \text{PH}_3 > \text{AsH}_3$.³⁰ (2) PAs increase as the polarizability and electron-donating ability of the alkyl group increase. Both effects stabilize the protonated species, RXH^+ . (3) The slopes of the lines in Figure 3 show that the PAs for alkyl halides are more sensitive to changes in the alkyl group than the PAs of amines and alcohols. As discussed previously,⁴ this is due to the greater carbonium ion character of the RXH^+ ($\text{R}^+\cdots\text{XH}$) ions than the ROH_2^+ or RNH_3^+ species, which is also manifested in smaller ΔE_s values for the protonated alkyl halides.

Finally, it is noted that the PAs for alkyl fluorides correlate with the total charge on the FH fragment in RFH^+ . For the 4-31G results, the relation is given in eq 8 using HF, CH_3F , $\text{C}_2\text{H}_5\text{F}$, and $(\text{CH}_3)_2\text{CHF}$ as the data points. The standard deviation is 1.9 kcal/mol. The apparent reason for the correlation can be attributed to the same factors as in point 2 above. Similar relations apply to primary amines, alcohols, and alkyl chlorides.⁴

$$\text{PA (4-31G)} = -179.22(q_F + q_H) + 180.53 \text{ kcal/mol} \quad (8)$$

Implications for Chemistry in Superacid Media

One of the motivations for studying the interactions of HF and carbonium ions is to eventually simulate the solvation of carbonium ions in superacid solutions via statistical mechanics techniques.³¹ HF is the simplest of the superacid solvents from a theoretical standpoint. Other common alternatives are SO_2 , SO_2ClF , and SO_2F_2 . In a typical experiment, carbonium ions are formed by hydride or halide abstraction from alkanes or alkyl halides using SbF_5 in liquid HF.^{3b} The superacid solvents



are all characterized by their weak nucleophilicity. For example, HF has a lower methyl cation affinity, ΔE_s , than N_2 .^{2a} Therefore, the low ΔE_s values found here for protonated fluorides were fully anticipated. The details of the results do, however, illuminate some other experimental observations.

First, "free" secondary and tertiary carbonium ions are well known to have been prepared in superacid solutions according to the usual NMR chemical shift criteria.³ This is consistent with the low ΔE_s values (<8 kcal/mol) that are reported here for *i*-PrFH⁺ and *t*-BuFH⁺. Furthermore, these weak solvent-ion interactions should yield little preference for the solvation of *isomeric* secondary or tertiary carbonium ions in superacid. Thus, Arnett's observation that the 2-butyl and *tert*-butyl cations have similar relative energies in SO_2ClF (14.5 kcal/mol) as in the gas phase (15–17 kcal/mol) is not surprising.³⁴ Differences in cavity formation in superacid for the isomeric ions apparently have little energetic impact. Also, ion pairing with SbF_6^- or $\text{Sb}_2\text{F}_{11}^-$ is probably not pronounced owing to the low nucleophilicity of the anions.

In contrast, free primary carbonium ions appear to be unknown in superacid. Gillespie has reported that CH_3^+ complexes with the solvent in all cases.^{32a} For example, dissolving CH_3F in $\text{SbF}_5/\text{SO}_2\text{ClF}$ yields $\text{CH}_3\text{OSOFCI}^+\text{Sb}_2\text{F}_{11}^-$ and in SbF_5/SO_2 the principal product is $\text{CH}_3\text{OSO}^+\text{Sb}_2\text{F}_{11}^-$. This behavior is consistent with the ΔE_s 's of 15–28 kcal/mol for the protonated primary fluorides treated here. Clearly, at least one solvated molecule would be anticipated to remain intimately associated with the primary carbonium ions at all times. Consequently, it is unlikely that a truly free C_2H_5^+ is the active agent in the alkylations of alkanes by ethylene in TaF_5/HF .^{32b}

Similarly, it appears doubtful that vinyl cations have been prepared in superacid, even aryl stabilized species, e.g., $(\text{CH}_3)_2\text{C}=\text{C}^+-\text{ArX}$.³³ Attempts at generating less stable ions would certainly be complicated by addition or complexation with the solvent since the ΔE_s for CH_3CHF^+ is 38 kcal/mol (Table IV).

Finally, the 4 kcal/mol weaker interaction of HF with the bridged ethyl cation than with its bisected isomer (Table IV) is consistent with earlier MINDO/3 calculations and perturbation theory arguments.^{4,19} As discussed above, more extensive calculations could well reduce the difference. Thus, this limited evidence suggests that solvent effects on the relative energies of isomeric carbonium ions in a *nonnucleophilic* medium such as superacid are slight.⁴

Conclusion

The present study has shown that insights into the gas-phase ion chemistry of fluoroalkanes can be obtained from ab initio calculations within the Hartree-Fock framework. Furthermore, the interactions of carbonium ions and HF in the gas phase were found to be consistent with observations in superacid media. Various correlations involving the properties of alkyl fluorides were also noted. This work completes a series of investigations on the properties and protonation of alkyl halides.⁴ Knowledge gained in these endeavors will, no doubt, prove valuable in future theoretical work on systems in condensed phases.³¹

Acknowledgments. The authors are grateful to Professor J. L. Beauchamp for helpful discussions and receipt of unpublished data. Acknowledgment is made to the donors of the Petroleum Research Fund, administered by the American

Chemical Society, for support of this work. Additional aid was provided by the Purdue University Computing Center.

References and Notes

- (1) Chemical Consequences of Orbital Interactions. 14. Part 13: ref 4b.
- (2) For representative studies of alkyl halides and their ions in the gas phase, see (a) J. L. Beauchamp, D. Holtz, S. D. Woodgate, and S. L. Paitt, *J. Am. Chem. Soc.*, **94**, 2798 (1972), and references cited therein; (b) K. C. Kim, J. H. Beynon, and R. G. Cooks, *J. Chem. Phys.*, **61**, 1305 (1974); (c) ref 8 and 9.
- (3) For reviews, see (a) G. A. Olah et al., *J. Am. Chem. Soc.*, **99**, 5683 (1977), and the preceding papers in this series; (b) D. M. Brouwer and H. Hogeveen, *Prog. Phys. Org. Chem.*, **9**, 179 (1972); (c) M. Saunders, P. Vogel, E. L. Hagen, and J. Rosenfeld, *Acc. Chem. Res.*, **6**, 53 (1973).
- (4) (a) W. L. Jorgensen, *J. Am. Chem. Soc.*, **100**, 1049 (1978); (b) *ibid.*, **100**, 1057 (1978); (c) W. L. Jorgensen and J. E. Munroe, *ibid.*, **100**, 1511 (1978); (d) W. L. Jorgensen, *Chem. Phys. Lett.*, **53**, 527 (1978).
- (5) (a) W. J. Hehre, R. F. Stewart, and J. A. Pople, *J. Chem. Phys.*, **51**, 2657 (1969); (b) R. Ditchfield, W. J. Hehre, and J. A. Pople, *ibid.*, **54**, 724 (1971).
- (6) GAUSSIAN/74 is a CDC version of GAUSSIAN/70: W. J. Hehre, W. A. Lathan, R. Ditchfield, M. D. Newton, and J. A. Pople, QCPE Program No. 236. The authors are grateful to Professor Pople and co-workers for kindly providing a copy of the program.
- (7) (a) J. E. DelBene and A. Baccaro, *J. Am. Chem. Soc.*, **98**, 7526 (1976); (b) M. D. Newton and S. Ehrenson, *ibid.*, **93**, 4971 (1971); (c) P. A. Kollman and S. Rothenberg, *ibid.*, **99**, 1333 (1977).
- (8) (a) A. D. Williamson, P. R. LeBreton, and J. L. Beauchamp, *J. Am. Chem. Soc.*, **98**, 2705 (1976); (b) J. L. Beauchamp and J. Y. Park, *J. Phys. Chem.*, **80**, 575 (1976).
- (9) (a) M. S. Foster and J. L. Beauchamp, *Inorg. Chem.*, **14**, 1229 (1975); (b) R. J. Blint, T. B. McMahon, and J. L. Beauchamp, *J. Am. Chem. Soc.*, **96**, 1269 (1974); (c) D. P. Ridge and J. L. Beauchamp, *ibid.*, **96**, 3595 (1974); (d) R. D. Wieting, R. H. Staley, and J. L. Beauchamp, *ibid.*, **96**, 7552 (1974); (e) R. H. Staley, R. D. Wieting, and J. L. Beauchamp, *ibid.*, **99**, 5964 (1977).
- (10) W. A. Lathan, L. A. Curtiss, W. J. Hehre, J. B. Lisle, and J. A. Pople, *Prog. Phys. Org. Chem.*, **11**, 175 (1974).
- (11) J. A. Pople and M. Gordon, *J. Am. Chem. Soc.*, **89**, 4253 (1967).
- (12) R. W. Taft, Jr., in "Steric Effects in Organic Chemistry", M. S. Newman, Ed., Wiley, New York, N.Y., 1956, p 619.
- (13) (a) A. D. Baker, D. Betteridge, N. R. Kemp, and R. E. Kirby, *Anal. Chem.*, **43**, 375 (1971); (b) L. S. Levitt and B. Levitt, *Tetrahedron*, **29**, 941 (1973); (c) T. P. Fehlner, J. Ulman, W. A. Nugent, and J. K. Kochi, *Inorg. Chem.*, **15**, 2544 (1976); (d) W. A. Nugent and J. K. Kochi, *J. Am. Chem. Soc.*, **98**, 5979 (1976).
- (14) Data from ref c, Table III. The dipole moment of *t*-BuBr has apparently not been determined.
- (15) For a review, see W. J. Hehre in "Applications of Electronic Structure Theory", H. F. Schaefer III, Ed., Plenum Press, New York, N.Y., 1977, p 277.
- (16) (a) J. F. Wolf, R. H. Staley, I. Koppel, M. Taagepera, R. T. McIver, Jr., J. L. Beauchamp, and R. W. Taft, *J. Am. Chem. Soc.*, **99**, 5417 (1977); (b) R. W. Taft in "Proton Transfer Reactions", E. Caldin and V. Gold, Ed., Chapman and Hall, London, 1975, p 31.
- (17) P. Kebarle, *Annu. Rev. Phys. Chem.*, **28**, 373 (1977).
- (18) P. A. Kollman and C. F. Bender, *Chem. Phys. Lett.*, **21**, 271 (1973).
- (19) Energies for STO-3G optimized structures of the carbonium ions are used to compute the ΔE_s 's.^{10,15} STO-3G geometries for the carbonium ions have been used rather than 4-31G because optimized structures for all the carbonium ions of interest here are only available at the STO-3G level.¹⁵
- (20) A PA of 94.3 kcal/mol for HF has recently been reported: C. Y. Nyg, D. J. Trevor, P. W. Tiedemann, S. T. Ceyer, P. L. Kronebusch, B. H. Mahan, and Y. T. Lee, *J. Chem. Phys.*, **67**, 4235 (1977). The discrepancy with Beauchamp's ICR value is disturbing and is not discussed by Lee et al. Concern may be expressed that the H_2F^+ generated by Lee et al. by photoionization of $(\text{HF})_2$ is excited. Additional experiments are warranted.
- (21) (a) W. L. Jorgensen and J. E. Munroe, *Tetrahedron Lett.*, **581** (1977); (b) P. C. Myhre and E. Evans, *J. Am. Chem. Soc.*, **91**, 5641 (1969).
- (22) For a review of theoretical studies of C_2H_5^+ , see D. Heldrich, M. Grimmer, and H.-J. Köhler, *Tetrahedron*, **32**, 1193 (1976).
- (23) D. T. Clark and D. M. J. Lilley, *Chem. Commun.*, **1042** (1970).
- (24) For a review, see K. Fukui, *Acc. Chem. Res.*, **4**, 57 (1971).
- (25) The drawing was produced by the PSI/77 program, QCPE No. 340, written by W. L. Jorgensen. The orbital value is 0.1 au.
- (26) It may be noted that 4 and 3 are fluorine analogues of keto-enol tautomers. The preference for 4 is similar to the 11.7 kcal/mol higher energy for vinyl alcohol than acetaldehyde that was recently reported from 4-31G calculations: W. J. Bouma, D. Poppinger, and L. Radom, *J. Am. Chem. Soc.*, **99**, 6443 (1977).
- (27) W. J. Hehre, R. Ditchfield, L. Radom, and J. A. Pople, *J. Am. Chem. Soc.*, **92**, 4796 (1970).
- (28) In this context, an extreme view would be that all single determinant calculations are inappropriate for the estimation of PAs and ΔE_s 's. The agreement with experiment that is obtained in studies like this one argues against such a brash position. However, some cancellation of errors must be occurring since for fluoroalkanes PAs are better estimated with 4-31G than STO-3G, while for chloroalkanes the opposite is true.
- (29) S. W. Benson, "Thermochemical Kinetics", Wiley, New York, N.Y., 1968, p 22.
- (30) D. Holtz, J. L. Beauchamp, and J. R. Eyler, *J. Am. Chem. Soc.*, **92**, 7045 (1970); R. H. Wyatt, D. Holtz, and J. L. Beauchamp, *Inorg. Chem.*, **13**, 1511 (1974).

- (31) To this end, an intermolecular potential function for $(\text{HF})_2$ has recently been determined from 6-31G computations: W. L. Jorgensen and M. E. Cournoyer, *J. Am. Chem. Soc.*, in press.
- (32) J.-Y. Calves and R. J. Gillespie, *J. Am. Chem. Soc.*, **99**, 1788 (1977); (b) M. Siskin, *ibid.*, **98**, 5413 (1976).
- (33) For a review, see M. Hanack, *Acc. Chem. Res.*, **9**, 364 (1976); M. Hanack, *ibid.*, in press.
- (34) E. W. Blitner, E. M. Arnett, and M. Saunders, *J. Am. Chem. Soc.*, **98**, 3734 (1976).
- (35) (a) W. J. Hehre and P. C. Hiberty, *J. Am. Chem. Soc.*, **96**, 2665 (1974); W. J. Hehre, J. A. Pople, and A. J. P. Devaquet, *ibid.*, **98**, 664 (1976); (b) the 4-31G energy for 4 reported here is slightly lower than Hehre's result because geometry optimization was only done at the STO-3G level in the earlier work.

Molecular Orbital Theory of the Hydrogen Bond. 20. Pyrrole and Imidazole as Proton Donors and Proton Acceptors

Janet E. Del Bene* and Irwin Cohen

Contribution from the Department of Chemistry, Youngstown State University, Youngstown, Ohio 44555. Received February 6, 1978

Abstract: Ab initio SCF calculations with a minimal STO-3G basis set have been performed to determine the structures and stabilization energies of hydrogen bonded pyrrole-water and imidazole-water complexes in which pyrrole and imidazole act either as proton donors or as proton acceptors. While imidazole is a stronger proton donor to water than pyrrole, both molecules form stronger N-H...O hydrogen bonds with water than are found in amide-water complexes. The structures of the pyrrole-water and imidazole-water dimers are similar, as are the nearby regions of the intermolecular potential surfaces. As proton acceptor molecules, pyrrole and imidazole are quite different. While imidazole forms a strong hydrogen bond with water through the nitrogen σ lone pair of electrons in the molecular symmetry plane, pyrrole forms a relatively weak and flexible π complex with water, with hydrogen bond formation occurring preferentially at the C₃-C₄ bond. The O-H...N hydrogen bond in the imidazole-water dimer is stronger than the O-H...N hydrogen bonds found in azine-water complexes, although the imidazole-water intermolecular potential surface in this region resembles the pyridimine-water potential surface. The π hydrogen bond in the pyrrole-water dimer is stronger than that in the ethylene-water dimer.

Introduction

In previous papers of this series,¹ the heterocyclic aromatic azines pyridine, pyridazine, pyrimidine, and pyrazine were investigated as proton acceptor molecules in hydrogen bonded complexes. Pyrrole and imidazole are two other small heterocyclic aromatic compounds which may also form hydrogen bonds, these by acting either as proton donor or as proton acceptor molecules. It is of interest to investigate the hydrogen bonding properties of these molecules to compare and contrast them with each other, with the azines and ethylene as proton acceptors, and with formamide and methyl-substituted formamides as proton donors. Since both pyrrole and imidazole rings are present in important biological systems, their characterization in dimers with water is a necessary first step toward characterizing and understanding their interactions through hydrogen bonding in these more complex systems.

In the present study, ab initio SCF calculations have been performed to determine the structures and stabilization energies of hydrogen bonded pyrrole-water and imidazole-water complexes, and to investigate the nature of the intermolecular potential surfaces surrounding these structures. It is the purpose of this paper to present the results of this study, and to compare pyrrole and imidazole with each other, with the amides as proton donors, and with the azines and ethylene as proton acceptors.

Method of Calculation

The closed-shell ground state wave functions for pyrrole and imidazole and their hydrogen bonded complexes with water have been described by single Slater determinants Ψ

$$\Psi = |\psi_1(1)\bar{\psi}_1(2)\dots\psi_n(2n-1)\bar{\psi}_n(2n)|/\sqrt{(2n)!}$$

constructed from doubly occupied molecular orbitals (MO's).

The MO's ψ_i are expressed parametrically as linear combinations of atomic basis functions ϕ_μ (the LCAO approximation)

$$\psi_i = \sum_{\mu} c_{\mu i} \phi_{\mu}$$

with the expansion coefficients $c_{\mu i}$ determined by solving the Roothaan equations.² The set of atomic basis functions used in this study is the minimal STO-3G basis set with standard scale factors.³ This basis set has been used previously for studies of hydrogen bonded complexes, thus permitting direct comparisons of computed results.

Because the use of nonoptimized monomer geometries can lead to spurious dimer stabilization,^{4,5} the first step in this investigation was to optimize the pyrrole and imidazole geometries. For pyrrole, C_{2v} symmetry was assumed, and bond lengths and bond angles were optimized cyclicly and independently to ± 0.01 Å and $\pm 1^\circ$, respectively. For imidazole, C_s symmetry was assumed, and bond distances and bond angles were again optimized as in pyrrole. The optimized STO-3G structure of water has been reported previously.⁶

With the constraint that the optimized monomer geometries remain rigid in the hydrogen bonded complexes,⁴ it is possible to describe the relative orientation of the pair of hydrogen bonded molecules in an intermolecular coordinate system in terms of an intermolecular distance R , and five intermolecular angles, defined with reference to an intermolecular line and the principal axes of the proton donor and proton acceptor molecules. For pyrrole, the principal axis has been chosen as the C_2 symmetry axis, coincident with the N-H bond, with origin at the nitrogen atom. For imidazole as a proton donor molecule, the principal axis has been chosen in a similar manner to be coincident with the N₁-H bond, with origin at